Analysis on Numerical Simulation of Large-Scale Structure

Weixuan Pan[1], Qiao Wang[2]

[1]*Astronomy Department, Guangzhou University*

[2]*National Astronomical Observatories of the Chinese Academy of Sciences*

We systematically investigate the influence of cosmological parameters on the matter power spectrum and the statistical properties of dark matter halos. We analyze the sensitivity characteristics of baryon density, cold dark matter density, and primordial perturbation amplitude on the matter power spectrum, finding that the three parameters respectively introduce oscillatory features at intermediate scales, exhibit strong scale dependence, and generate a scale-independent scaling effects. Based on N-body simulations, we employ the Friends-of-Friends algorithm to identify dark matter halos. Through analysis of mass function, density profile, and two-point correlation function, we find that the Watson empirical formula and the Einasto profile best characterize the statistical properties of dark halos, and our simulation results are highly consistent with the predictions of theoretical dark halo models.

1   Introduction

One of the core tasks of modern cosmology is to understand the evolutionary process of matter distribution in the universe and the formation mechanism of large-scale structures. The ΛCDM standard model provides us with a basic theoretical framework for describing cosmic evolution [1] [2] [3] [4]. This model successfully explains the cosmic expansion revealed by Hubble's law, the isotropic characteristics of the cosmic microwave background radiation, and the observed light element abundances consistent with the Big Bang nucleosynthesis theory. Within this standard model framework, large-scale structures in the universe are believed to originate from the gravitational instability growth of primordial density perturbations. These tiny perturbations gradually amplify during cosmic evolution, ultimately forming the complex hierarchical cosmic structures we observe today.

The matter power spectrum is a fundamental quantity describing the statistical properties of density perturbations in the universe, carrying comprehensive cosmological information from the cosmic microwave background to the large-scale distribution of galaxies. Different cosmological parameters produce significant and distinctive effects on the shape and amplitude of the power spectrum, making the matter power spectrum an important observational probe for constraining cosmological parameters and testing theoretical models. A deep understanding of how cosmological parameters modulate the detailed features of the power spectrum is crucial for accurately extracting cosmological information from observational data.

In the hierarchical picture of cosmic structure formation, dark matter halos play a vital role. According to the current theoretical framework, baryonic matter accumulates and cools within the gravitational potential wells of dark matter halos, ultimately forming observable structures such as galaxies. Therefore, dark matter halos serve not only as the key link connecting cosmological theory with observational phenomena, but also as the foundation for understanding the physical processes of galaxy formation and evolution. Characteristics such as the mass distribution, internal density structure, and spatial clustering patterns of dark matter halos directly reflect the physical nature of nonlinear structure formation in the universe, providing important observational constraints for verifying cosmological models and deeply understanding gravitational dynamic processes.

As fundamental building blocks of large-scale structure in the universe, the statistical properties and internal structural characteristics

of dark matter halos play a central role in modeling structure formation and evolution. First, the dark halo mass function describes the number density distribution of halos with different masses, directly reflecting the nonlinear evolution process of density perturbations. Halo density profiles reveal the clustering patterns of dark matter under gravitational influence, providing constraints for understanding the dynamical equilibrium within halos. The spatial clustering properties of halos are associated with the clustering patterns of large-scale structure, representing an important pathway to understand the history of matter aggregation in the universe.

2 Standard Cosmological Model

The ΛCDM cosmological model, also known as the standard cosmological model, achieves its success to three key observational facts: Hubble's law confirming cosmic expansion, the cosmic microwave background radiation from the early universe, and the abundances of light elements consistent with Big Bang nucleosynthesis. As the theoretical cornerstone of modern cosmology, the standard cosmological model provides a framework for our understanding of the large-scale structure and evolution of the universe.

2.1 Robertson-Walker Metric

The cosmological principle assumes that the universe is homogeneous and isotropic on large scales. This principle has been validated by observations of the large-scale homogeneous distribution of galaxies and the highly isotropic cosmic microwave background radiation. To satisfy this symmetry in spacetime, we use the Robertson-Walker metric for representation.

According to the cosmological principle, we can conduct mathematical analysis of the geometric properties of space. If there is no special property at every point in space, the curvature of space should be equal everywhere, meaning that space has constant curvature.

We first consider the simple case of a two-dimensional spherical surface. The spherical equation is

$$x_1^2 + x_2^2 + x_3^2 = R^2 \qquad (1)$$

By differentiating the spherical surface equation and substituting it into the distance formula between two points on the spherical surface, we can obtain

$$dl^2 = R^2 \left(\frac{dr^2}{1 - r^2} + r^2 d\theta^2 \right) \qquad (2)$$

Now imagine the expansion of our universe as analogous to the inflation of a balloon surface. That is, consider our three-dimensional space as a "three-dimensional surface" in four-dimensional space, which gives

$$dl^2 = R^2 \left(\frac{dr^2}{1 - r^2} + r^2 d\theta^2 + r^2 \sin^2 \theta d\varphi^2 \right) \qquad (3)$$

Adding the time dimension, we get

$$ds^2 = dt^2 - a^2(t) \times \left(\frac{dr^2}{1 - kr^2} + r^2 d\theta^2 + r^2 \sin^2 \theta \, d\phi^2 \right) \qquad (4)$$

Here we use a to replace R because the universe expands with time, so a is a function of time. This is the famous Robertson-Walker metric. The advantage of the Robertson-Walker metric lies in its simplicity: it is completely determined by a curvature constant k and a function R(t) that reflects the curvature radius. It must be emphasized that the R-W metric is derived solely from the cosmological principle, requiring no other physical assumptions or additional conditions. It is a purely kinematic metric. If we wish to study the dynamical evolution of the universe, we must consider other physical models, such as general relativity. Substituting the Robertson-Walker metric into the Einstein equation, we can obtain the basic equation for studying cosmological models, that is, the Friedmann Equations.

2.2 Friedmann Equations

By substituting the energy-momentum tensor of a perfect fluid into Einstein's field equations and employing the R-W metric, we obtain

$$\left(\frac{\dot{a}}{a}\right)^2 = \frac{8\pi G}{3}\rho + \frac{\Lambda}{3} - \frac{k}{a^2} \qquad (5)$$

This is the general form of the Friedmann Equations. One side of the equation tells us how the structure of the universe will expand or contract over time. The other side of the equation includes all forms of matter, radiation, and any other energy forms that make up the universe. It also includes the intrinsic curvature of space (different curvatures correspond to different shapes of the universe). It even includes the cosmological constant (denoted by "Λ") that Einstein introduced into the equation to maintain a static universe.

3 The Matter Power Spectrum

The matter power spectrum is a fundamental quantity describing the statistical properties of density perturbations in the universe, encompassing comprehensive information from the cosmic microwave background to large-scale structure formation. Understanding how different cosmological parameters influence the shape and amplitude of the power spectrum is crucial for accurately extracting cosmological information from observational data [5]. As shown in Figure 1, we analyze the impact of cosmological parameters on the matter power spectrum.

Figure 1 demonstrates the influence of three key cosmological parameters on the matter power spectrum and their sensitivity analysis. The upper panels show the absolute matter power spectrum $P(k)$ under different parameter values, while the lower panels display the fractional deviations relative to the baseline model, providing important insights into understanding how each parameter affects structure formation at different scales.

The left panel investigates the impact of the baryon density parameter $\Omega_b h^2$. As seen in the upper figure, when $\Omega_b h^2$ increases from 0.012 to 0.032, the matter power spectrum exhibits relatively mild changes on large scales, but differences gradually emerge on small scales. The residual plot below more clearly reveals this scale dependence: on large scales ($k < 10^{-2}$ h/Mpc), the deviations caused by different $\Omega_b h^2$

values are relatively small and vary smoothly; around intermediate scales, particularly near the characteristic scale of baryon acoustic oscillations, obvious oscillating patterns appear, reflecting the acoustic oscillation history of the baryon-photon fluid before recombination; on small scales, an increase in baryon density leads to a systematic enhancement of the power spectrum, mainly due to the contribution of baryonic matter to the total matter density.

The middle panel displays the effects of the cold dark matter density parameter $\Omega_c h^2$. Unlike baryon density, variations in cold dark matter density produce more significant and systematic effects on the matter power spectrum. The upper plot shows that as $\Omega_c h^2$ increases, the power spectrum amplitude rises across the entire k range, directly reflecting the role of dark matter as the primary driving force for structure formation. Residual analysis reveals an interesting scale-dependent characteristic: on large scales, higher $\Omega_c h^2$ values lead to significant enhancement of the power spectrum, with deviations reaching over 40%; as the scale decreases, this influence gradually weakens; on extremely small scales, the deviation approaches a constant value. This behavioral pattern reflects the differential contribution of dark matter to structure formation at different scales—large-scale structure formation depends more on the total amount of dark matter, while small-scale structures are more regulated by nonlinear evolutionary processes.

The right panel analyzes the influence of the primordial scalar perturbation amplitude A_s. As the key parameter determining the initial conditions of perturbations, A_s exhibits the most intuitive characteristics in its effect on the matter power spectrum. The upper plot shows that variations in A_s cause an overall vertical translation of the entire power spectrum, which aligns with expectations from linear perturbation theory, since the power spectrum is proportional to the square of the perturbation amplitude. The residual plot further confirms this: across the entire k range, the fractional deviation remains essentially constant, indicating that changes in A_s affect all scales proportionally. Specifically, when A_s increases from 1.5×10^{-9} to 2.5×10^{-9},
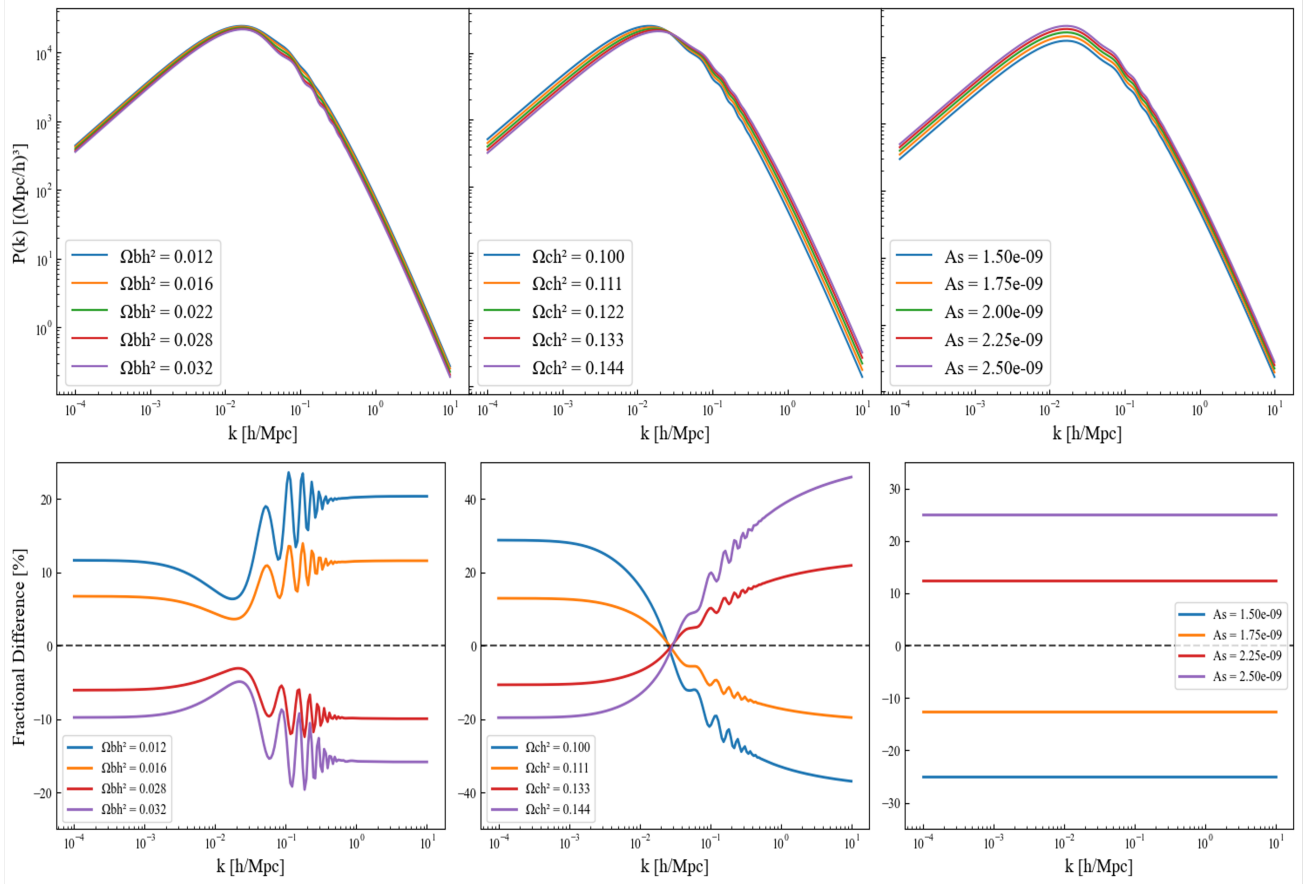
Figure 1: Matter power spectrum sensitivity to cosmological parameters. The top figures show the effects of three cosmological parameters on the amplitude and shape across different scales. The bottom figures illustrate fractional deviations from fiducial values, highlighting parameter-specific signatures at various wavenumbers.

the relative change in the power spectrum is approximately 25% at all scales. This scale-independent property makes A_s the primary determinant of the overall normalization of the power spectrum.

By comparing the impact patterns of the three parameters, we can find that each has unique "fingerprint" characteristics. Baryon density mainly generates oscillating features on intermediate scales, cold dark matter density exhibits strong scale dependence, and the primordial perturbation amplitude produces scale-independent overall scaling effects. These different sensitivity patterns provide an important theoretical basis for the observational constraints on cosmological parameters. By measuring the matter power spectrum at different scales, we can effectively separate and constrain these fundamental cosmological parameters, thereby gaining deep insights inot the com-

position and evolutionary history of the universe.

4 Dark Matter Halo Properties and Clustering Statistics

After matter became dominant in the universe, density perturbations of non-baryonic matter first grew rapidly. Perturbations that meet certain conditions eventually collapse to form dark halos. After baryonic matter decoupled from radiation, its density perturbations grew rapidly under the gravitational influence of non-baryonic matter. Baryonic matter cooled and collapsed within dark halos, ultimately forming the various structures observed in the universe today. Based on theoretical speculations and observational verifications (such as galaxy rotation curves and gravitational lensing effects), we generally believe that galaxies form within
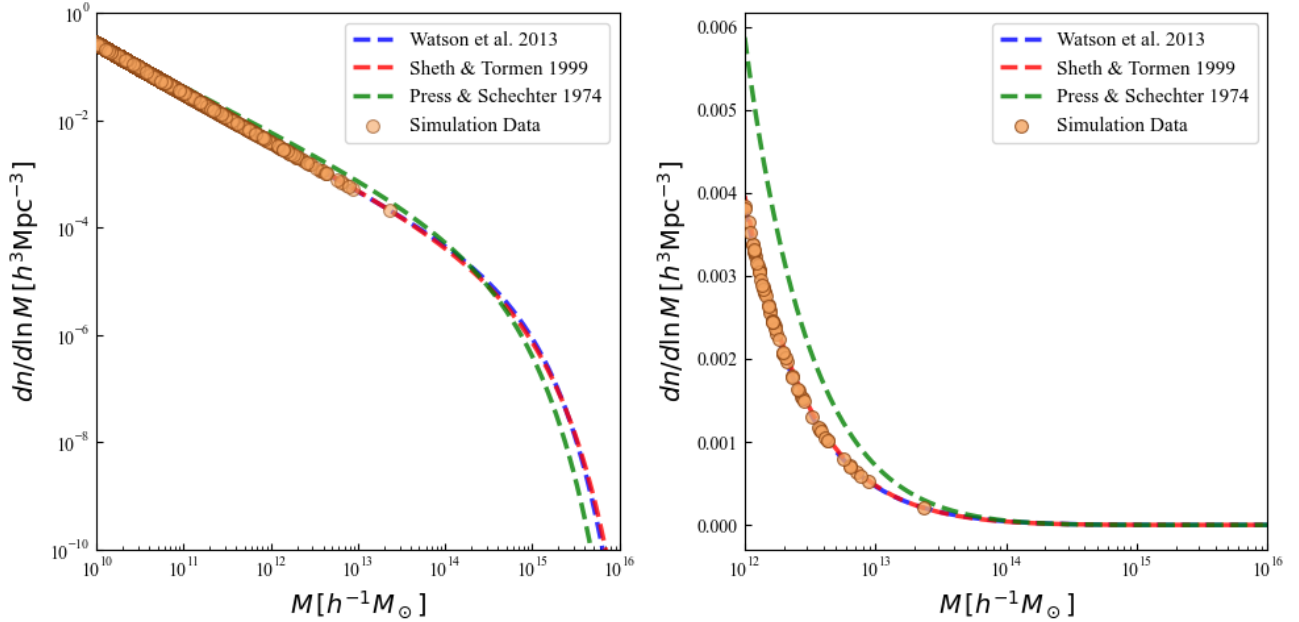
Figure 2: Halo mass function models comparison. The blue dashed line represents the empirical fitting formula by Watson et al., the red dashed line shows the modified model by Sheth & Tormen, the green dashed line indicates the classical Press & Schechter model, and the orange circles represent dark matter halos identified by the FoF algorithm.

dark halos. The establishment of dark halo models has built a convenient bridge for research connecting cosmic density fields to galaxy formation theory, greatly advancing the study of galaxy formation theory. Therefore, dark matter halos are a fundamental feature of large-scale structures. Research on dark halos can deepen our understanding of galaxy evolution, and studies on galaxies can in turn constrain the properties of dark halos, thereby constraining dark matter models.

4.1 Halo Mass Function

The halo mass function (HMF) is a characteristic property of cosmic structure formation models, used to quantify the number density of dark matter halos per unit mass in the universe. This function is crucial for understanding the distribution of matter in the universe and helps connect cosmological parameters with observable structures, thus deepening our understanding of cosmic structure formation and evolution.

We extracted three-dimensional coordinate data for 30 million dark matter particles from snapshot files of N-body cosmological simulations. These data are stored in HDF5 format

files, with a simulation box size of $50\,h^{-1}Mpc$. To optimize computational efficiency, we employed a random sampling strategy, randomly selecting 1 million particles from all particles as our sample. Through constructing a KDTree spatial index and considering periodic boundary conditions, we calculated the average distance between particles and used 0.2 times the average distance as the linking length. We then applied the Friends-of-Friends algorithm to identify 2 million dark matter halo structures.

In the mass function analysis, we adopted Planck 2018 cosmological parameters [6] and used the colossus library [7] to calculate three different theoretical halo mass function models: the Watson et al. empirical fitting formula [8], the Sheth & Tormen modified model [9], and the classic Press & Schechter model [10]. We compared the dark matter halos extracted from simulation data with these theoretical predictions.

The analysis results are shown in Figure 2. The left panel displays the complete mass range comparison, while the right panel focuses on details at the low-mass end, with the horizontal axis representing logarithmic mass and the vertical axis showing the mass function val-

ues in linear scale. In this more detailed display, we can observe distinct differences between the three theoretical models at the low-mass end: the Press & Schechter model (green dashed line) gives higher predicted values at low masses, while the Sheth & Tormen and Watson et al. models (blue dashed lines) provide predictions that are relatively more consistent with the simulation. This result verifies that the Press & Schechter model has a relatively large error in describing the distribution of dark matter halos at this mass scale [11] [12].

4.2 Halo Density Profile

The Halo Density Profile is a fundamental physical quantity describing the spatial distribution of dark matter inside halos, reflecting the aggregation law of dark matter particles under gravitational action. This profile not only reveals the internal structural characteristics of dark matter halos but also provides key observational constraints for verifying the ΛCDM cosmological model and understanding the process of nonlinear structure formation. This profile not only reveals the internal structural characteristics of dark matter halos, but also provides crucial observational constraints for verifying ΛCDM cosmological models and understanding nonlinear structure formation processes.

Based on the previously identified dark matter halos, we selected the 10 most massive halos for analysis. To ensure the analysis accuracy, we implemented multiple halo center determination methods for comparative validation. In addition to traditional center-of-mass calculation methods, we introduced median-based approaches to reduce the influence of anomalous particles, as well as density peak methods that calculate the mass center of the innermost 1% of particles to more precisely locate the halo's gravitational center. This multi-method validation strategy effectively resolved systematic error issues in halo center positioning.

Coordinate unit correction is a key technical step in our entire analysis process. We systematically tested unit conversion factors of 1.0, 1000.0, and 2000.0 times, calculated the ratio of the maximum particle distance to the theoretical virial radius for each case, and selected the optimal parameter that kept this ratio fall within the physically reasonable range (0.3 - 0.8). This diagnosis process ensured the physical meaning and numerical stability of subsequent density profile calculations.

We adopted an improved algorithm design to calculate radial density profiles. We first computed the three-dimensional Euclidean distance from each particle to the halo center, then established 15 logarithmically spaced spherical shell binning structures in the radial direction. Inside each spherical shell, the density was calculated through the ratio of the number of particles, article mass, and shell volume, i.e., $\rho = (N_{particles} m_{particle})/V_{shell}$. To ensure data quality, our algorithm automatically removed data points with zero density or containing invalid values, and retained only statistically significant radial intervals.

In the theoretical comparative analysis, we integrated two main density profile models in dark matter halo research. We took the NFW profile [13] [14] as a classic model developed based on numerical simulations, with its functional form being $\rho(r) = \rho_s/[(r/r_s)(1 + r/r_s)]$, which has been verified across a wide range of masses and redshifts. We also considered the Einasto profile [15], which provides a more flexible empirical description and usually shows better fitting accuracy in the outer regions of halos. We used the mass - concentration relation from Duffy et al. [16] to estimate the concentration parameter of each halo, and this parameter is crucial for the normalization and shape of the theoretical profile.

The final visualization results are shown in Figure 3. Both models can reasonably well describe the internal density structure of dark matter halos but show subtle differences within different radius ranges. This analysis verified the accuracy of N-body simulations in reproducing the internal structure of dark matter halos and provided quantitative basis for understanding the density distribution characteristics of dark matter halos with different masses.
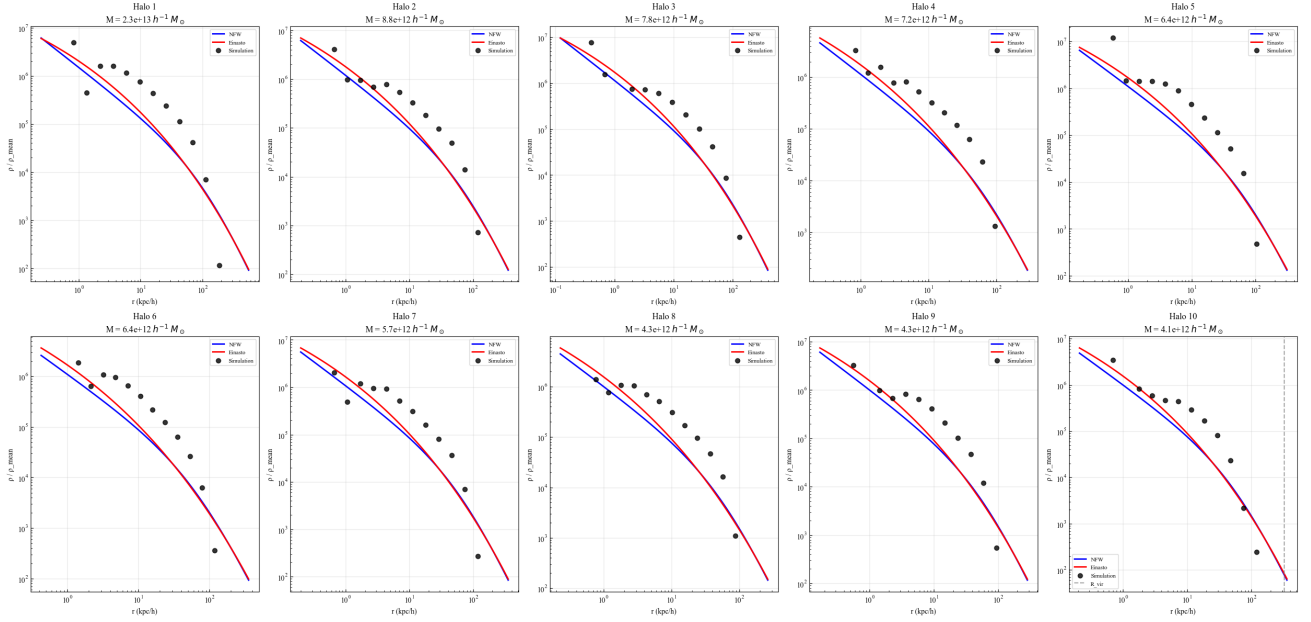
Figure 3: Density profile characteristics across different mass scales. Each panel corresponds to a dark matter halo of specific mass. The black scatter points represent the actual density profiles computed from our simulation data, while the blue and red curves show the predictions from NFW and Einasto theoretical models, respectively.

4.3 Halo Two-Point Correlation Function

The two-point correlation function (2PCF) is a statistical tool for quantifying the spatial clustering degree of dark matter halos, describing the enhanced probability of finding two halos beyond random distribution at a given separation distance. This function directly reflects the clustering mode of dark matter halos in large-scale structure and provides crucial statistical constraints for verifying cosmological models and understanding nonlinear structure formation.

The general framework for the two-point correlation function can be expressed as

$$\xi(r) = \xi^{1h}(r) + \xi^{2h}(r) \tag{6}$$

Among them, $\xi^{1h}(r)$ represents the 1 - halo term and is expressed as

$$\xi^{lh}(r) = \frac{1}{\rho^2} \int dM \, M^2 n(M)$$
$$\times \int d^3\vec{g} \, u(\vec{x} - \vec{y}|M) \tag{7}$$
$$\times u(\vec{x} + \vec{r} - \vec{y}|M)$$

$\xi^{2h}(r)$ represents the 2 - halo term, involving the correlation between different dark matter halos, and is expressed as

$$\xi^{2h}(r) = \frac{1}{\rho^2} \int dM_1 \, M_1 b(M_1) n(M_1)$$
$$\times \int dM_2 \, M_2 b(M_2) n(M_2)$$
$$\times \int d^3\vec{y}_1 \int d^3\vec{y}_2 \, u(\vec{x} - \vec{y}_1|M_1)$$
$$\times u(\vec{x} + \vec{r} - \vec{y}_2|M_2)\xi_{gm}^{lin}(\vec{y}_1 - \vec{y}_2) \tag{8}$$

In the above formulas, $\bar{\rho}$ represents the cosmic mean density, $n(M)$ is the halo mass function, $b(M)$ is the halo bias factor, $u(\vec{x}|M)$ is the halo density profile, and $\xi_{mm}^{lin}(r)$ is the linear dark matter two-point correlation function.

We first used the halomod and hmf packages [17] [18] to establish the theoretical framework based on TracerHaloModel, employing the Eisenstein-Hu transfer function [19] and Zehavi05 HOD model [20] to calculate the theoretically predicted two-point correlation function. In the theoretical calculations, we set key HOD parameters including minimum halo mass $M_{min} = 12.5$, satellite halo mass $M_1 = 13.5$, and slope index $\alpha = 1.0$. These parameters control the occupation probabilities of central galaxies and satellite galaxies in dark matter halos.
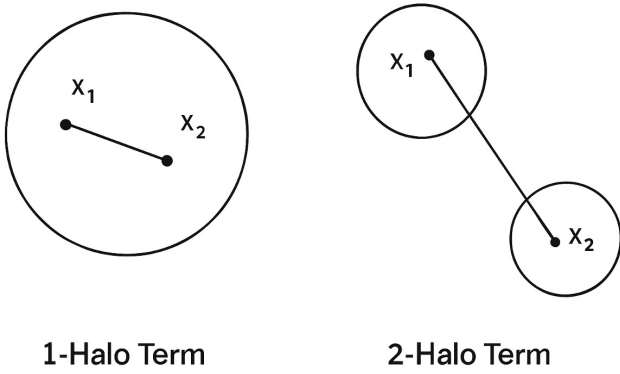
Figure 4: 1-halo vs 2-halo terms. The 1-halo term describes the correlation between particle pairs within the same dark matter halo and dominates on small scales, while the 2-halo term reflects the large-scale correlations between different dark matter halos.
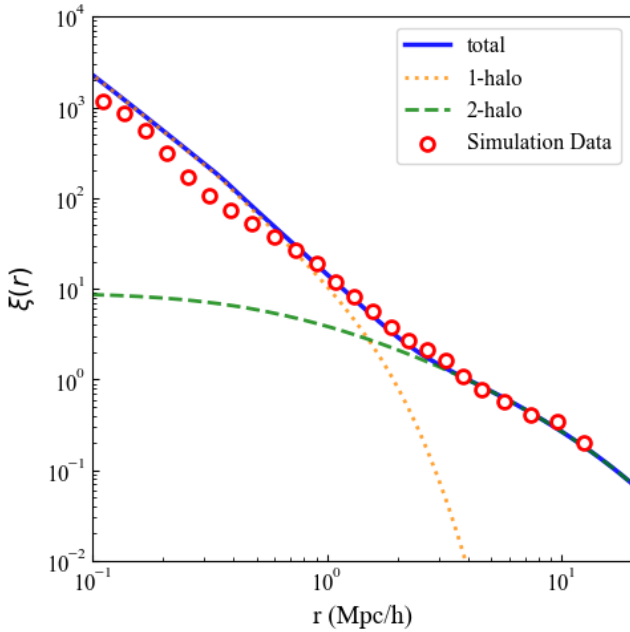

Figure 5: Halo two point correlation function. The figure includes the total theoretical correlation function (blue solid line), the 1-halo term theoretical prediction (orange dotted line), the 2-halo term theoretical prediction (green dashed line), and the simulation data points (red open circles).

In simulated data processing, to optimize the computational accuracy and efficiency of the correlation function, we designed an adaptive directional binning strategy. This strategy employs dense sampling at small scales to capture strong clustering signals, employs moderate density sampling at intermediate scales, and sparse sampling at large scales to reduce noise effects.

We used the tpcf function from the halotools packages [21] to calculate the two-point correlation function of simulation data, adopted Natural estimator and considered periodic boundary conditions, and finally obtained correlation function measurement values for 24 radial bins.

Through the visualization analysis and quantitative comparison in Figure 5, we found that the simulation results show good consistency with theoretical predictions across most scale ranges. This validates the physical description of the 1h term to 2h term transition region, confirming the effectiveness of large-scale linear clustering theory. The 1-halo term dominates at small scales, reflecting the strong nonlinear dynamical processes inside halos, while the 2-halo term contributes to the linear density fluctuation growth and halo bias effects at large scales. This analysis not only validates the accuracy of N-body simulations in reproducing dark matter halo spatial distribution statistical properties, but also provides quantitative evidence for understanding different physical processes at different spatial scales, thereby offering important observational constraints for galaxy formation and large-scale structure evolution theories.

5 CONCLUSION

Based on N-body numerical simulations, we systematically analyzed the statistical properties and structural characteristics of dark matter halos. We employed the FoF algorithm to identify dark matter halo groups, and through mass function analysis, density profile studies, and two-point correlation function calculations, we explored the physical properties of dark matter halos. The results show that the Watson empirical formula and the Einasto profile exhibit the best precision in describing the mass distribution and density profile, while HOD models can effectively predict the clustering behavior of dark matter halos. In our study of cosmological parameter effects, we found that $\Omega_b h^2$, $\Omega_c h^2$ and

A_s have significant and unique scale-dependent impacts on the matter power spectrum, providing important theoretical foundations for cosmological parameter constraints.

Limited by computing resources, the size of the simulation box used in this study was only $50\,h^{-1}Mpc$. This relatively small size may affect the precision of large-scale statistical analysis, especially when studying rare massive halos and ultra-large-scale clustering patterns. We anticipate that future research will adopt larger-scale simulation data to obtain more reliable statistical results.

Acknowledgments

References

[1] P. J. E. Peebles, "Tests of cosmological models constrained by inflation," *ApJ*, vol. 284, pp. 439–444, Sep. 1984.

[2] D. N. Spergel, L. Verde, H. V. Peiris, E. Komatsu, M. R. Nolta, C. L. Bennett, M. Halpern, G. Hinshaw, N. Jarosik, A. Kogut, M. Limon, S. S. Meyer, L. Page, G. S. Tucker, J. L. Weiland, E. Wollack, and E. L. Wright, "First-Year Wilkinson Microwave Anisotropy Probe (WMAP) Observations: Determination of Cosmological Parameters," *ApJS*, vol. 148, no. 1, pp. 175–194, Sep. 2003.

[3] E. Komatsu, K. M. Smith, J. Dunkley, C. L. Bennett, B. Gold, G. Hinshaw, N. Jarosik, D. Larson, M. R. Nolta, L. Page, D. N. Spergel, M. Halpern, R. S. Hill, A. Kogut, M. Limon, S. S. Meyer, N. Odegard, G. S. Tucker, J. L. Weiland, E. Wollack, and E. L. Wright, "Seven-year Wilkinson Microwave Anisotropy Probe (WMAP) Observations: Cosmological Interpretation," *ApJS*, vol. 192, no. 2, p. 18, Feb. 2011.

[4] C. S. Frenk and S. D. M. White, "Dark matter and cosmic structure," *Annalen der Physik*, vol. 524, no. 9-10, pp. 507–534, Oct. 2012.

[5] M. P. van Daalen, J. Schaye, C. M. Booth, and C. Dalla Vecchia, "The effects of galaxy formation on the matter power spectrum: a challenge for precision cosmology," *MNRAS*, vol. 415, no. 4, pp. 3649–3665, Aug. 2011.

[6] Planck Collaboration, N. Aghanim et al., "Planck 2018 results. VI. Cosmological parameters," *A&A*, vol. 641, p. A6, Sep. 2020.

[7] B. Diemer, "COLOSSUS: A Python Toolkit for Cosmology, Large-scale Structure, and Dark Matter Halos," *ApJS*, vol. 239, no. 2, p. 35, Dec. 2018.

[8] W. A. Watson, I. T. Iliev, A. D'Aloisio, A. Knebe, P. R. Shapiro, and G. Yepes, "The halo mass function through the cosmic ages," *MNRAS*, vol. 433, no. 2, pp. 1230–1245, Aug. 2013.

[9] R. K. Sheth and G. Tormen, "Large-scale bias and the peak background split," *MNRAS*, vol. 308, no. 1, pp. 119–126, Sep. 1999.

[10] W. H. Press and P. Schechter, "Formation of Galaxies and Clusters of Galaxies by Self-Similar Gravitational Condensation," *ApJ*, vol. 187, pp. 425–438, Feb. 1974.

[11] P. Valageas, "Mass functions and bias of dark matter halos," *A&A*, vol. 508, no. 1, pp. 93–106, Dec. 2009.

[12] Z. J. Xu, "Dark matter halo mass functions and density profiles from mass and energy cascade," *Scientific Reports*, vol. 13, p. 16531, Oct. 2023.

[13] J. F. Navarro, C. S. Frenk, and S. D. M. White, "The Structure of Cold Dark Matter Halos," *ApJ*, vol. 462, p. 563, May 1996.

[14] J. F. Navarro, C. S. Frenk, and S. D. M. White, "A Universal Density Profile from Hierarchical Clustering," *ApJ*, vol. 490, no. 2, pp. 493–508, Dec. 1997.

[15] J. Einasto, "On the Construction of a Composite Model for the Galaxy and on the Determination of the System of Galactic Parameters," *Trudy Astrofizicheskogo Instituta Alma-Ata*, vol. 5, pp. 87–100, Jan. 1965.

[16] A. R. Duffy, J. Schaye, S. T. Kay, and C. Dalla Vecchia, "Dark matter halo concentrations in the Wilkinson Microwave Anisotropy Probe year 5 cosmology," *MNRAS*, vol. 390, no. 1, pp. L64–L68, Oct. 2008.

[17] S. G. Murray, C. Power, and A. S. G. Robotham, "HMFcalc: An online tool for calculating dark matter halo mass functions," *Astronomy and Computing*, vol. 3, p. 23, Nov. 2013.

[18] S. G. Murray, B. Diemer, Z. Chen, A. G. Neuhold, M. A. Schnapp, T. Peruzzi, D. Blevins, and T. Engelman, "THE-HALOMOD: An online calculator for the halo model," *Astronomy and Computing*, vol. 36, p. 100487, Jul. 2021.

[19] D. J. Eisenstein and W. Hu, "Baryonic Features in the Matter Transfer Function," *ApJ*, vol. 496, no. 2, pp. 605–614, Mar. 1998.

[20] I. Zehavi, Z. Zheng, D. H. Weinberg, M. R. Blanton, N. A. Bahcall, A. A. Berlind, J. Brinkmann, J. A. Frieman, J. E. Gunn, R. H. Lupton, R. C. Nichol, W. J. Percival, D. P. Schneider, R. A. Skibba, M. A. Strauss, M. Tegmark, and D. G. York, "Galaxy Clustering in the Completed SDSS Redshift Survey: The Dependence on Color and Luminosity," *ApJ*, vol. 736, no. 1, p. 59, Jul. 2011.

[21] A. P. Hearin, D. Campbell, E. Tollerud, P. Behroozi, B. Diemer, N. J. Goldbaum, E. Jennings, A. Leauthaud, Y.-Y. Mao, S. More, J. Parejko, M. Sinha, B. Sipöcz, and A. Zentner, "Forward Modeling of Large-scale Structure: An Open-source Approach with Halotools," *AJ*, vol. 154, no. 5, p. 190, Nov. 2017.